

Wollastonite from calc-silicates of the Kerala Khondalite Belt, southern India: Changing fluid regimes during deep crustal metamorphism

M. Satish-Kumar*, M. Santosh*, ** and M. Yoshida*

*Department of Geosciences, Faculty of Science, Osaka City University, Osaka 558, Japan

**Centre for Earth Science Studies, P B 7250, Akkulam, Thiruvikkal Post, Trivandrum 695 031, India

Orthopyroxene and wollastonite are critical minerals in the end-member models on granulite petrogenesis in the Earth's deep crust, and are considered to be mutually incompatible. We report here the occurrence, mineralogy and chemistry of wollastonites from calc-silicates in a number of new localities of the Kerala Khondalite Belt, southern India, where they are associated with orthopyroxene-bearing charnockites. While the charnockite mineral phase equilibria constrain $X_{\text{CO}_2} > 0.85$ to drive the orthopyroxene-forming reaction, the presence of wollastonite in the calc-silicates requires X_{CO_2} to be < 0.25 . We provide mineral reaction and fluid inclusion evidence which suggests that wollastonite formation occurred under low X_{CO_2} conditions during the prograde sector of a clockwise P-T path, whereas orthopyroxene stability and charnockite formation resulted under anhydrous conditions through the structurally controlled influx of CO_2 along an isothermal decompression path. The wollastonite- and orthopyroxene-bearing assemblages described in this study have important implications in evaluating changing fluid regimes during deep crustal metamorphism.

THE nature and role of fluids in granulite facies environment have been topics of debate, as they are crucial in evaluating the lower crustal and crust-mantle interaction processes^{1,2}. The stability of granulite facies minerals changes drastically with respect to change in fluid composition. For example, while orthopyroxene is stable only under anhydrous conditions, the stability of wollastonite requires hydrous environment. Therefore, wollastonite and orthopyroxene are considered to be incompatible under the same pressure-temperature-fluid (P-T-X) conditions³.

The southern Indian granulite facies terrain has been central to the debate on the role of fluids in granulite genesis, especially anhydrous charnockites, and is regarded as a critical example of fluid-controlled granulite formation. The stability of anhydrous mineral assemblages, particularly the presence of orthopyroxene in the charnockitic rocks in this terrain, is generally ascribed to dehydration induced by the influx of CO_2 -rich fluids

from sublithospheric sources⁴⁻⁷. The presence of arrested charnockites, i.e. patch and vein type of granulites developed within upper amphibolite facies gneisses, in many parts of the terrain have been cited as evidence for the external influx of CO_2 -rich fluids^{8,9}. Quite contrary to this, granulite facies rocks in some other terrains, such as the Adirondacks in North America, have provided evidence for CO_2 -absent (fluid-free) environment. These terrains principally associate calc-silicates particularly with the index mineral wollastonite¹⁰⁻¹².

In this study, we report the occurrence of wollastonite from a number of calc-silicate localities in the Kerala Khondalite Belt in southern India. Importantly, in most cases, the calc-silicates are associated with orthopyroxene-bearing charnockites. These occurrences, therefore, constitute unique examples to evaluate diverse fluid processes within the same crustal segment.

Calc-silicates in the KKB

The Kerala Khondalite Belt (KKB) represents a vast supracrustal sequence metamorphosed to the upper amphibolite to granulite facies. The dominant lithologies in KKB are garnet- and sillimanite-bearing aluminous granulites (khondalites), garnet- and biotite-bearing upper amphibolite facies gneisses (leptynites), and garnet- and orthopyroxene-bearing anhydrous granulites (charnockites). Interlayered with these, pyroxene granulites, quartzites and calc-silicates occur in subordinate amounts. The regional pressure-temperature conditions as estimated from mineral phase equilibria and fluid inclusion thermobarometers lie in the range of $700 \pm 50^\circ\text{C}$ and $5 \pm 1 \text{ kbar}$ ^{7,13}. Charnockite formation in the KKB is exemplified by the patch, vein and lensoid development of granulite facies assemblages along mesoscopic faults and shears within garnet biotite gneisses, and has been linked to the channelled influx of CO_2 through structural pathways from sublithospheric sources^{2,7,8}. The fluid influx has also been shown to have resulted in the precipitation of isotopically heavy graphites in several localities¹⁴.

Calc-silicates in the Kerala Khondalite Belt occur as

minor lithological units as in other granulite facies terrains (e.g. Australia¹¹, Antarctica¹², Eastern Ghats¹⁵, Sri Lanka¹⁶). They form thin bands of varying thickness ranging from less than 1 m to more than 100 m. They occur as concordant layers commonly adjacent to charnockites. The common mineral assemblage of these rocks is wollastonite + scapolite + clinopyroxene \pm garnet \pm calcite \pm quartz \pm sphene \pm graphite. Pressure-temperature conditions calculated from equilibrium mineral assemblages in the calc-silicates are concordant with the regional P-T regime of the terrain (Satish-Kumar *et al.*, in preparation). The calc-silicates also show textural evidence for metamorphic uplift along an isothermal decompression path similar to the cordierite-bearing granulites of KKB¹⁷. Unlike some of the examples in other terrains¹², garnet is conspicuously absent in many of the KKB calc-silicates, which also supports an isothermal P-T evolution for the terrain.

Mineralogy and chemistry of KKB wollastonites

Localities where wollastonite-bearing calc-silicates have been identified in this study are shown in Figure 1,

and their salient field and mineralogical features are summarized in Table 1.

Wollastonite in the KKB calc-silicates can be grouped into two types based on the field relations: the granular type and the vein type. Granular type occurs as polygonal to tabular grains in textural equilibrium with other phases such as clinopyroxene and scapolite. The veins and seams of wollastonite (e.g. Sankaramugham, cf. Figure 1, Table 1) cut across the banding of calc-silicates. Wollastonite from both examples can be identified in hand specimen by its brittle and fibrous character developed due to the pronounced prismatic cleavage, white to greyish-white colour and low hardness. In thin section, the wollastonites show elongated tabular nature, low birefringence and straight extinction. In terms of the optical properties, the two types of wollastonites are indistinguishable. It is observed that all the wollastonites in the KKB occur as discrete primary phase, as against the wollastonite coronas identified from some other granulite facies terrains¹². The common associated minerals are clinopyroxene, scapolite, quartz and calcite.

Pure wollastonite crystals were hand-picked under a binocular microscope from crushed calc-silicate samples, and X-ray diffraction studies were carried out using a Rigaku X-ray powder diffractometer housed at the Osaka City University (CuK α target). The *d* spacings (cf. Table 2) correspond well with the range reported for the JCPDS standard (Table 2), and the wollastonite polytype is identified as triclinic ITr.

We carried out electron microprobe analysis of wollastonite from different locations in the KKB using a JEOL-MX 8600 Superprobe housed at the University of Kochi, Japan. The analyses were done with an accelerating voltage of 15 kV and a beam diameter of 2–3 μ m. Both natural and synthetic standards were used and oxide ZAF correction performed throughout. The analytical results are summarized in Table 3. Wollastonites in KKB are almost pure, and their chemistry compares well with that of wollastonites from other granulite terrains. The CaO and SiO₂ contents vary only marginally, and FeO and MnO are present only in minor amounts.

Orthopyroxene and wollastonite-forming reactions

Wollastonite-bearing calc-silicates in the KKB are often closely associated with orthopyroxene-bearing charnockites (cf. Table 1). In a typical example at Nuliyam (locality 1 in Figure 1 and Table 1), garnet- and biotite-bearing upper amphibolite facies gneisses show complete charnockitization at the contact with the calc-silicate layer, grading to incipient charnockites away from the contact¹⁸. Phase equilibria studies show that orthopyroxene formation in the charnockite occurred

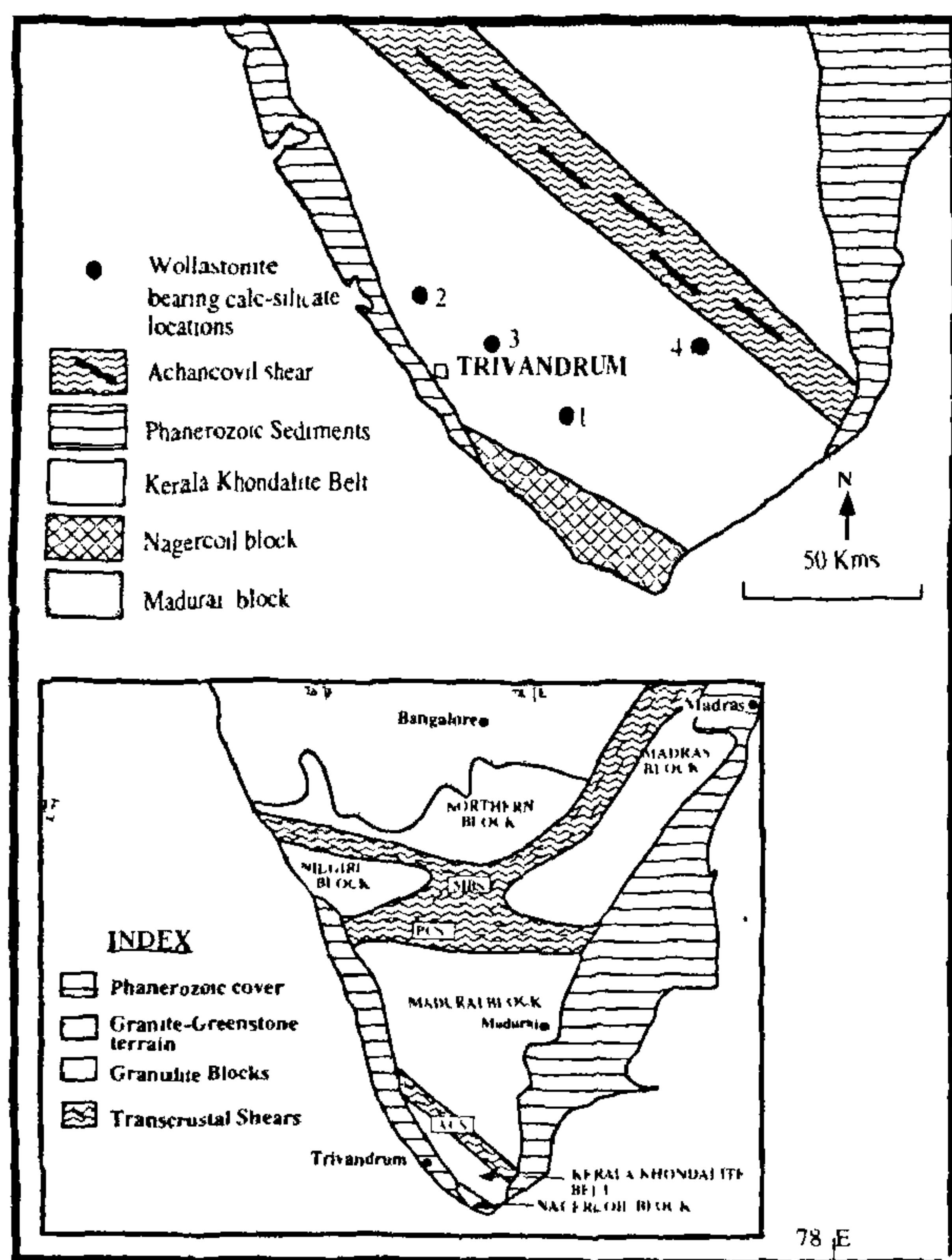


Figure 1. Generalized geological map of the Kerala Khondalite Belt showing the wollastonite-bearing calc-silicate locations reported in this study. Locations 1 – Nuliyam, 2 – Korani; 3 – Sankaramugham; 4 – Ambasarnudram. Inset shows the tectonic framework of the granulite terrain of South India.

Table 1. Field and mineralogical features of wollastonites from the Kerala Khondalite Belt, South India

Location number (cf. Figure 1)	Name of locality	Mineral assemblage	Associated rock type	Wollastonite type
1	Nuliyam	Wollastonite + diopside + scapolite \pm K-feldspar \pm calcite \pm quartz \pm graphite	Massive charnockite grading to incipient away from calc-silicate contact	Granular and vein type
2	Korani	Wollastonite + diopside + scapolite + plagioclase \pm K-feldspar \pm calcite \pm quartz	Massive charnockite	Granular
3	Sankaramugham	Wollastonite + diopside + scapolite + plagioclase \pm K-feldspar \pm calcite \pm grossular \pm quartz	Metapelite khondalite	Granular and vein type
4	Ambasamudram	Calcite + phlogopite + diopside \pm wollastonite \pm tremolite \pm humite \pm scapolite \pm graphite	Garnet-biotite gneiss (leptynite) showing incipient charnockitization	Granular and vein type

Table 2. XRD data of wollastonites from the KKB

Sample no.	1	2	3	4	JCPDS
2 θ	26° 50''	26° 56''	26° 48''	26° 40''	
	23° 10''	23° 08''	23° 10''	23° 12''	
	25° 20''	25° 16''	25° 20''	25° 18''	
<i>d</i> spacing	3.322	3.315	3.327	3.322	3.314
	3.839	3.845	3.839	3.834	3.83
	3.516	3.525	3.516	3.52	3.51

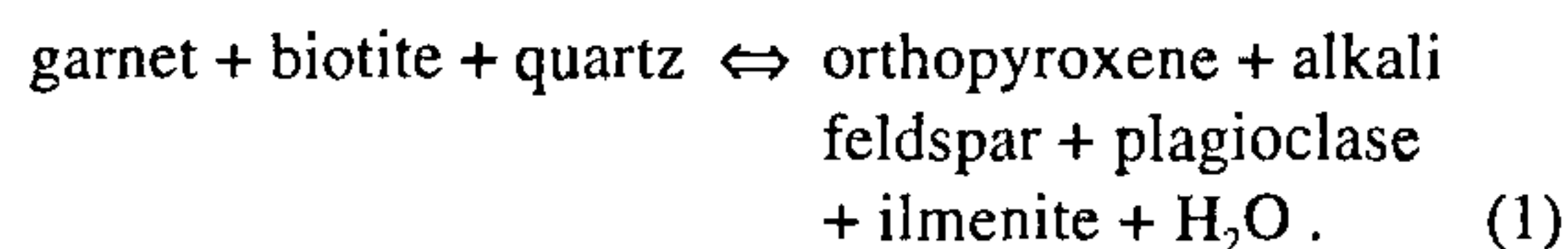
Table 3. Representative microprobe analysis of wollastonite

Location no.	1	1	3	4	2	2
SiO ₂	51.84	51.84	50.91	51.88	51.07	51.20
TiO ₂	0.04	0.04	0.00	0.00	0.00	0.03
Al ₂ O ₃	0.03	0.01	0.03	0.00	0.02	0.02
Cr ₂ O ₃	0.02	0.02	0.01	0.00	0.00	0.00
Fe ₂ O ₃	0.00	0.41	0.62	0.00	1.01	0.59
FeO	0.90	0.43	0.00	0.38	0.00	0.00
MnO	0.06	0.08	0.36	0.14	0.09	0.08
MgO	0.06	0.03	0.01	0.04	0.04	0.00
CaO	47.48	47.86	47.73	47.86	47.51	47.71
Na ₂ O	0.03	0.03	0.02	0.02	0.04	0.01
K ₂ O	0.00	0.00	0.01	0.01	0.00	0.00
Total	100.46	100.75	99.70	100.33	99.78	99.64

Cations on the basis of 6 oxygen atoms

Si	1.999	1.994	1.983	2.001	1.985	1.991
Ti	0.001	0.001	0.000	0.000	0.000	0.001
Al	0.001	0.000	0.001	0.000	0.001	0.001
Cr	0.001	0.001	0.000	0.000	0.000	0.000
Fe ³⁺	0.000	0.012	0.018	0.000	0.030	0.017
Fe ²⁺	0.029	0.014	0.000	0.012	0.000	0.000
Mn	0.002	0.003	0.012	0.004	0.003	0.003
Mg	0.003	0.001	0.001	0.002	0.002	0.000
Ca	1.961	1.972	1.992	1.978	1.978	1.987
Na	0.002	0.002	0.001	0.001	0.003	0.000
K	0.000	0.000	0.001	0.001	0.000	0.000
SCat	4.000	4.000	4.009	3.999	4.001	4.000

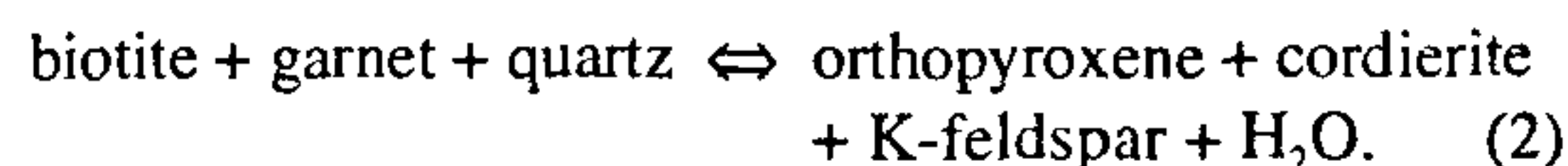
through dehydration induced by the influx of CO₂ according to the following reaction:



The X_{CO_2} required to stabilize this reaction is computed to be >0.85 [ref. 18].

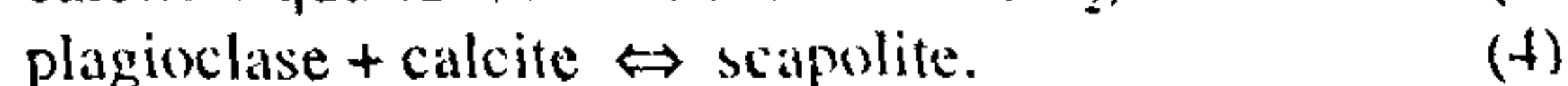
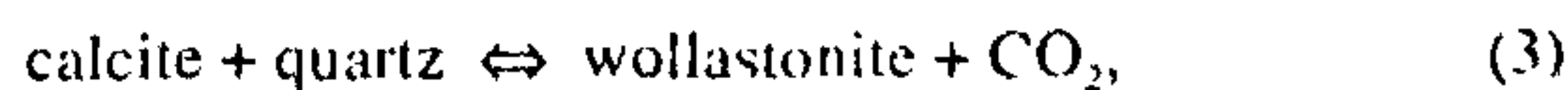
An identical dehydration reaction involving the breakdown of garnet, biotite and quartz to produce orthopyroxene has been proposed for incipient charnockite formation in different localities of the KKB⁷⁻⁹.

In localities where the bulk Mg/Fe composition of the host metapelite was high, cordierite is also recognized as a product phase along with orthopyroxene, according to the following reaction:



Cordierite- and orthopyroxene-bearing charnockites occurring as vein and patch assemblages within garnet-biotite gneisses adjacent to the Achankovil shear zone in the northern margin of the KKB are considered to have resulted from the above reaction¹⁹. Reaction (1) and (2) are essentially dehydration reactions, and under the pressure-temperature conditions defined for charnockite formation, the $X_{\text{H}_2\text{O}}$ should be of the order of 0.2–0.3 in order for these reactions to proceed^{7, 18, 19}.

On the other hand, the peak metamorphic assemblages in the calc-silicates of KKB indicate the following major reactions:



The presence of wollastonite in the calc-silicates requires low X_{CO_2} conditions. The stability of wollastonite itself provides a constraint on the maximum X_{CO_2} through the reaction (3) above. At granulite facies pressure-temperature conditions the wollastonite-bearing mineral

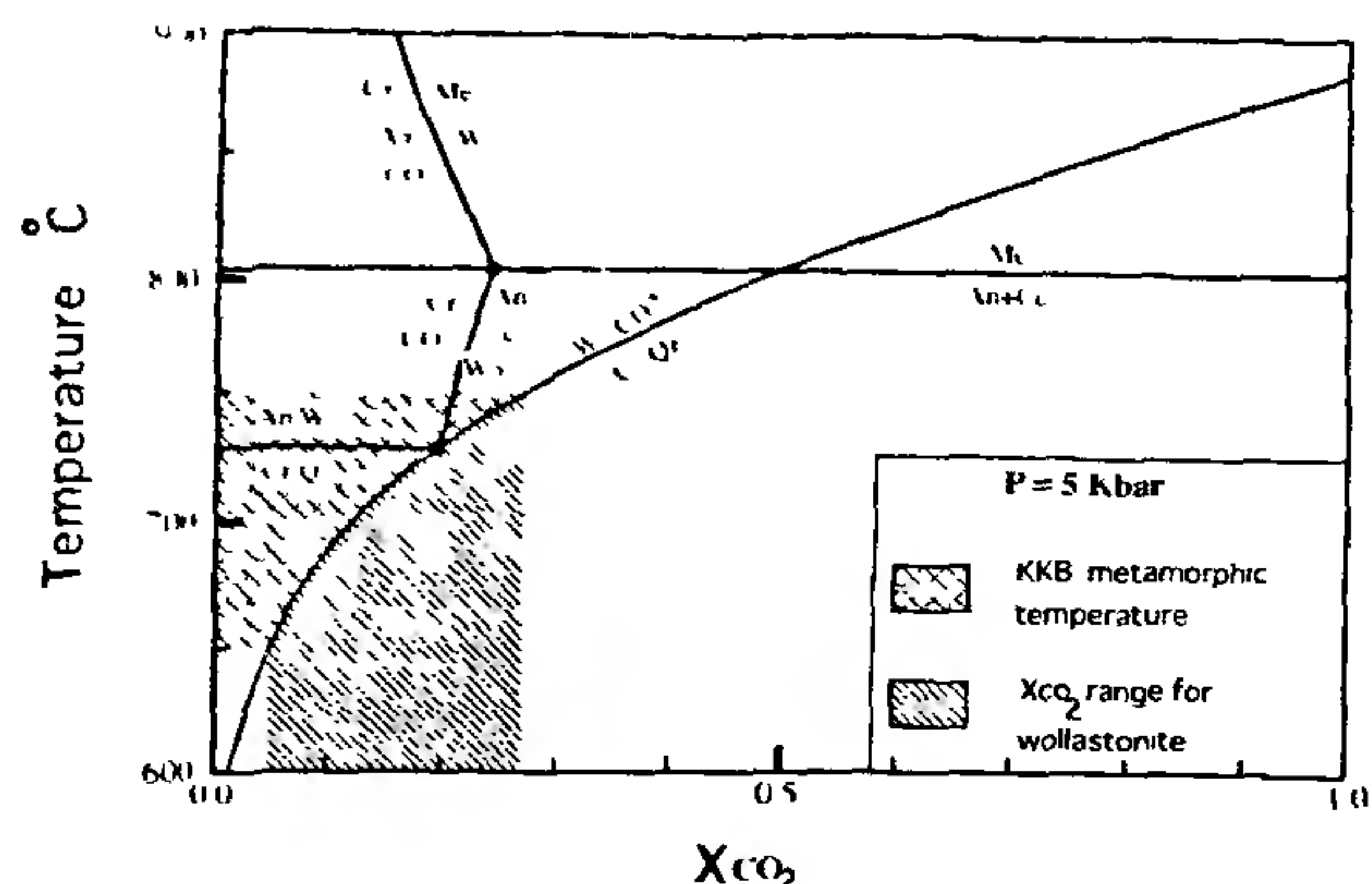


Figure 2. T - X_{CO_2} diagram of the relevant mineral phases in the system $\text{CaO-Al}_2\text{O}_3\text{-SiO}_2\text{-vapour}$ at 5 kbars (ref. 27)

assemblages will be stable in the presence of a fluid phase only if X_{CO_2} was around 0.25. This is further demonstrated in Figure 2, where the phase equilibria relations show that wollastonite and CO_2 are incompatible under normal pressure-temperature conditions recorded from different granulites. At high temperatures and low pressures, wollastonite can be stable at high X_{CO_2} conditions. At $700 \pm 50^\circ\text{C}$ and 5 kbar, which is the general estimate for KKB⁷, wollastonite stability requires the X_{CO_2} to lie between 0.1 and 0.22 (Figure 2). Also, it should be noted that wollastonite and scapolite cannot coexist at higher temperatures, and would react to form grossular. Grossular-forming reactions are high-temperature decarbonation reactions²⁰, and the absence of such reactions in the KKB suggests that the calc-silicates did not act as CO_2 sources at peak metamorphism.

Calc-silicates in the KKB host a variety of peak/post-peak metamorphic reaction textures. Some of these reactions post-date the granoblastic and layered fabrics of the main regional metamorphism. Most important for this study is reaction (3) above. In almost all cases, textural studies reveal that wollastonite, already formed

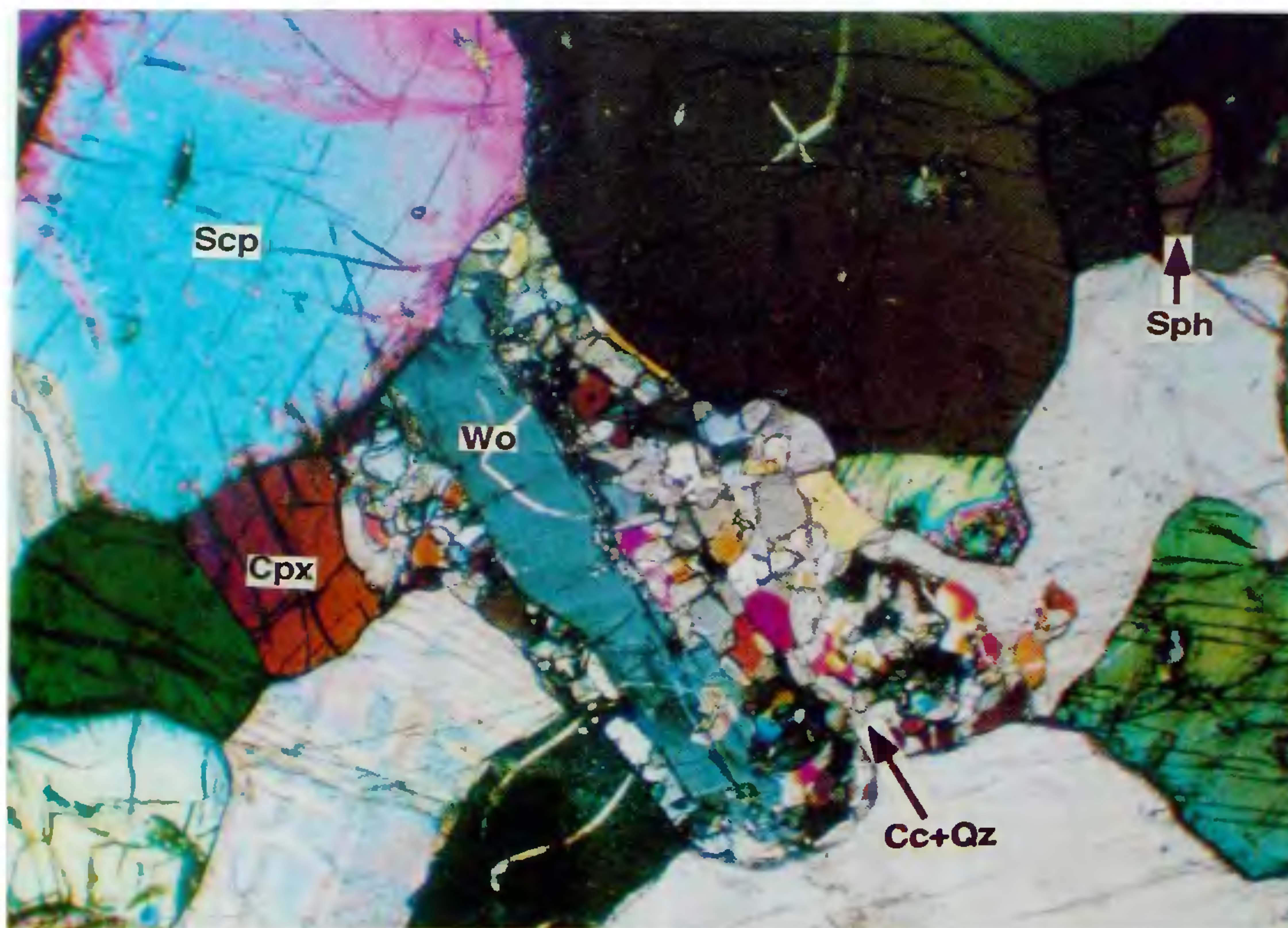


Figure 3a. Photomicrograph showing wollastonite (Wo) retrogressed to fine-grained calcite (Cc) and quartz (Qtz) assemblage. Associated minerals are scapolite (Scp), clinopyroxene (Cpx), calcite (Cc) and sphene (Sph). Note that wollastonite and scapolite do not react to form grossular. The length of the photograph measures 5 mm.

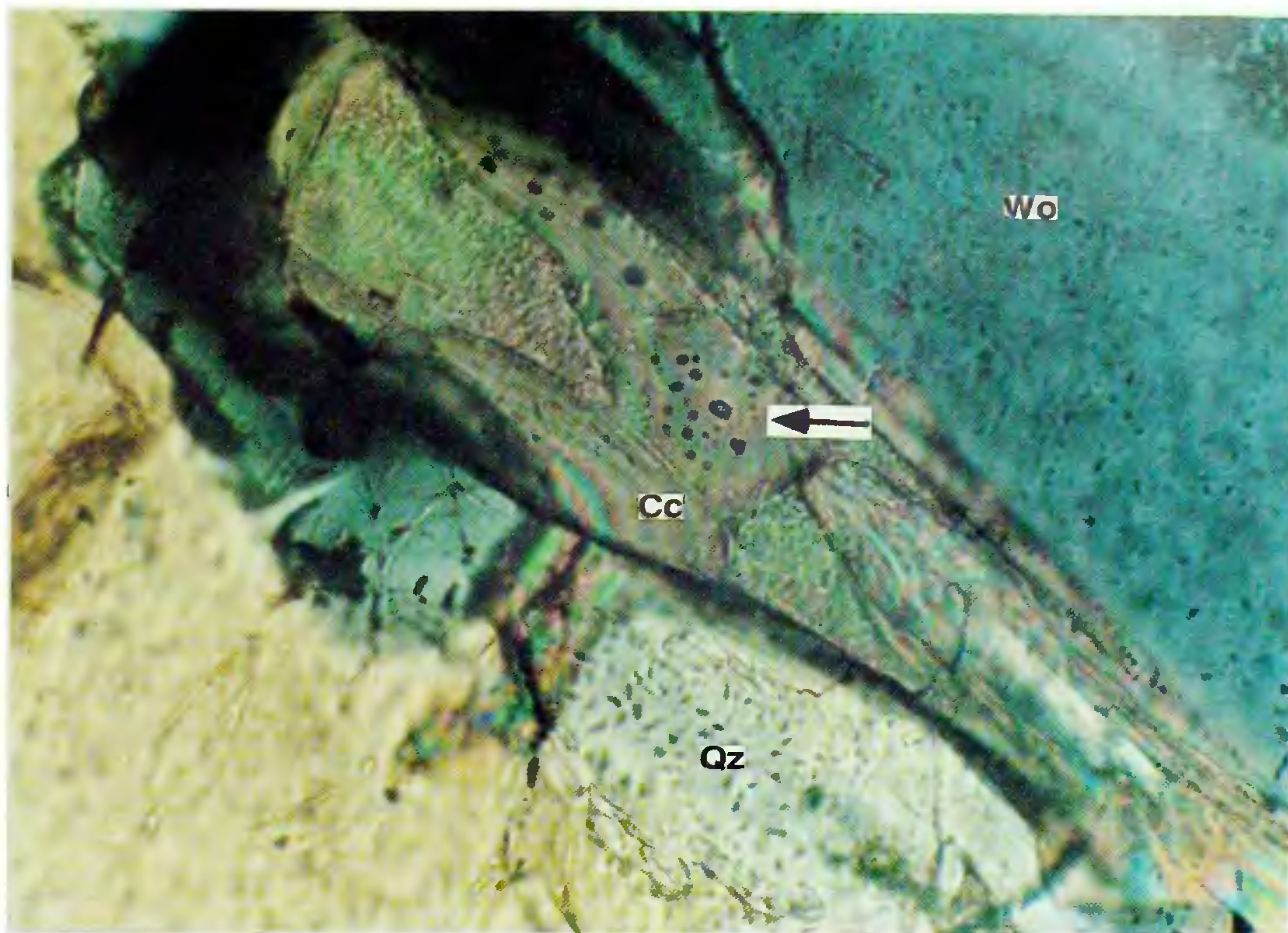
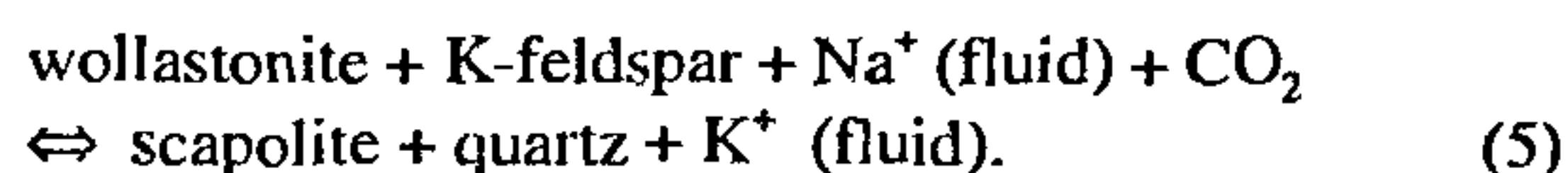


Figure 3b. High-density CO₂-rich inclusions (arrow) associated with retrogressed calcite. Mineral abbreviations as in Figure 3a. The length of the photograph measures 1 mm.

during prograde metamorphism, is partially retrogressed to an assemblage of fine-grained calcite and quartz along grain boundaries (Figure 3a), indicating the reverse reaction (1), where wollastonite breaks down to calcite and quartz in the presence of CO₂. Interestingly, fluid inclusion studies reveal that such retrogressed areas associate trapped CO₂-rich fluids (Figure 3b).

Another important reaction texture displayed by the calc-silicates involve scapolite + quartz symplectites separating K-feldspar and wollastonite, suggesting the following reaction²¹:



These textures collectively indicate that calc-silicates of the KKB evidenced the external influx of CO₂ subsequent to the formation of wollastonite.

Discussion

While CO₂-rich fluid inclusions associated with orthopyroxene-bearing charnockites from southern India

have been cited as examples for syn-metamorphic fluid influx⁷, the CO₂-rich fluid inclusions found in the wollastonite-bearing granulites of Adirondack Mountains in North America support post-metamorphic fluid infiltration³. Thus, orthopyroxene and wollastonite have been central to the debate over the timing and significance of fluid influx in granulite facies metamorphism and, consequently, the fluid processes in general in the Earth's lower crust.

Wollastonite- and scapolite-bearing assemblages in granulite terrains have recently been identified to be of critical importance in constraining the pressure-temperature-fluid histories, based on mineral reactions and textural characteristics¹². In crustal sections which have undergone isobaric cooling, garnet coronas commonly replace wollastonite-scapolite boundaries¹², whereas the reverse is often found in terrains characterized by clockwise P-T paths, where the rocks act as CO₂ sinks in the prograde sector²⁰. The KKB calc-silicates show pronounced absence of garnet-participating reactions, and the wollastonite retrogression is most probably brought about by external influx of fluids. These wollastonites display characteristic retrogression at grain boundaries

into calcite and quartz (cf. Figure 3a). This suggests that X_{CO} has been enhanced during the cooling history of the terrain. High-density CO_2 -rich fluid inclusions observed in quartz as well as calcite associated with these wollastonites support this inference (Satish-Kumar *et al.*, in preparation).

An important problem arising from the above observation is the timing of fluid infiltration, nature of fluids and mechanism of fluid transfer. Field evidence, importantly the association of wollastonite-bearing calc-silicates with orthopyroxene-bearing charnockites in the KKB, is indicative of varying fluid conditions in adjacent lithounits, as wollastonite in the calc-silicate and hypersthene in the charnockite cannot be stabilized together in the same fluid condition at a given P-T environment.

A possible explanation could be that wollastonite formed under regional metamorphism, and that CO_2 infiltration and charnockite formation were post-peak, which occurred during isothermal uplift along a decompressional path. The infiltration of carbonic fluids, which was instrumental in charnockite formation, was essentially structurally controlled^{7,8}. The characteristic grain boundary retrogression in wollastonites from the KKB suggests that CO_2 infiltration was not copious enough to achieve complete retrogression. The possible reason for this is that calc-silicates often act as permeability barriers in fluid infiltration, that is, they act as fluid guides rather than fluid sources or pathways²¹. From the textural and mineralogic evidence of wollastonites in calc-silicates of the KKB, it can be inferred that the fluids were largely internally buffered during peak metamorphism, and that channelled CO_2 infiltration occurred during the post-peak event, when the terrain underwent isothermal uplift.

It can be argued that wollastonite formation in the calc-silicate and orthopyroxene formation in the charnockite belong to two discrete metamorphic events. However, recent isotope geochronological data rule out this possibility. Sm-Nd and Rb-Sr mineral isochron studies from the regional metapelites (leptynites and khondalites) south of the Achankovil shear zone in the KKB, including the massive charnockites of the Nagercoil Block in the southern tip of Peninsular India, record a major Pan-African tectonothermal event, with regional metamorphism and terrain-wide rejuvenation²²⁻²⁴, Sm-Nd mineral isochron ages of ca. 540 Ma and Rb-Sr mineral isochron ages of ca. 470 Ma were obtained from the metapelites of the KKB in a recent study²³, which closely compare with the Pan-African ages for incipient charnockite formation reported from the KKB as well as the adjacent terrains in Sri Lanka²³⁻²⁵. All these studies confirm that incipient charnockite formation occurred along the post-peak decompressional uplift path, when CO_2 -rich fluids were introduced from external sources through structural pathways.

In accordance with the above, we interpret that wollastonite formation in the calc-silicate and charnockitization of the adjacent gneisses occurred during the same Pan-African regional metamorphic event, but under varying fluid regimes. While wollastonite in the calc-silicate was stabilized under hydrous conditions during the prograde path of a clockwise P-T trajectory, orthopyroxene crystallization and charnockite formation occurred under anhydrous conditions during the structurally controlled influx of CO_2 -rich fluids at the post-peak metamorphic stage, along the isothermal decompression segment of the P-T trajectory. One of the vital evidences for external CO_2 influx is that charnockite formation is also accompanied by graphite precipitation and the heavier carbon-enriched stable isotopic signature of these graphites clearly attest to crystallization from fluids²⁶.

1. Harley, S. L., *Geol. Mag.*, 1989, **126**, 215-247
2. Santosh, M., *J. Geol. Soc. India*, 1992, **39**, 375-399.
3. Lamb, W. M., Valley, J. W. and Brown, P. E., *Contrib. Mineral. Petrol.*, 1987, **96**, 485-495.
4. Newton, R. C., Smith, V. B. and Windley, B. F., *Nature*, 1980, **288**, 45-50.
5. Janardhan, A. S., Newton, R. C. and Hansen, E. C., *Contrib. Mineral. Petrol.*, 1982, **79**, 130-149.
6. Hansen, E. C., Janardhan, A. S., Newton, R. C., Prame, W. K. B. M. and Ravindrakumar, G. R., *Contrib. Mineral. Petrol.*, 1987, **96**, 225-244.
7. Santosh, M., Harris, N. B. W., Jackson, D. H. and Matthey, D. P., *J. Geol.*, 1990, **98**, 915-926.
8. Santosh, M., Jackson, D. H., Harris, N. B. W. and Matthey, D. P., *Contrib. Mineral. Petrol.*, 1991, **108**, 318-330.
9. Raith, M. and Srikantappa, C., *J. Metamorphic Geol.*, 1993, **11**, 815-832.
10. Lamb, W. M. and Valley, J. W., *Nature*, 1984, **312**, 56-58.
11. Warren, R. G., Hensen, B. J. and Ryburn, R. J., *J. Metamorphic Geol.*, 1987, **5**, 213-223.
12. Harley, S. L. and Buick, I. S., *J. Petrol.*, 1992, **33**, 693-728.
13. Chacko, T., Ravindrakumar, G. R. and Newton, R. C., *J. Geol.*, 1987, **95**, 343-358.
14. Santosh, M. and Wada, H., *J. Geol.*, 1993, **101**, 643-651.
15. Dasgupta, S., *J. Metamorphic Geol.*, 1993, **11**, 193-202.
16. Hoeffbauer, R. and Spiering, B., *Precamb. Res.*, 1994, **66**, 325-349.
17. Santosh, M., *Contrib. Mineral. Petrol.*, 1987, **96**, 616-651.
18. Jackson, D. H. and Santosh, M., *J. Metamorphic Geol.*, 1992, **10**, 365-382.
19. Santosh, M., Jackson, D. H. and Harris, N. B. W., *J. Petrol.*, 1993, **34**, 233-258.
20. Harley, S. L., Fitzsimons, I. S. W. and Buick, I. S., *Precamb. Res.*, 1994, **66**, 309-323.
21. Harley, S. L. and Santosh, M., *Contrib. Mineral. Petrol.*, 1994, in press.
22. Choudhary, A. K., Harris, N. B. W., Van Clasteren, P. C. and Hawkesworth, C., *J. Geol. Mag.*, 1992, **129**, 257-264.
23. Unnikrishnan-Warrier, C., Santosh, M. and Yoshida, M., *J. Geol. Soc. India*, 1995, in press.
24. Unnikrishnan-Warrier, C., Santosh, M. and Yoshida, M., *Geol. Mag.*, in press.
25. Burton, K. W. and O'Nions, R. K., *Contrib. Mineral. Petrol.*, 1990, **106**, 66-89.
26. Santosh, M. and Wada, H., *Earth Planet. Sci. Lett.*, 1993, **119**, 19-26.
27. Moecher, D. P. and Essene, E. J., *J. Petrol.*, 1990, **31**, 997-1024.

ACKNOWLEDGEMENTS We thank Dr S. Yoshikura for extending facilities for electron microprobe analyses. This study was funded by MONBUSHO Research Fellowship to the senior author and forms a part of his doctoral research. M. Santosh was supported by a Visiting Professorship at the Osaka City University, Japan. The Director, Centre for Earth Science Studies, Trivandrum, is acknowledged for

encouragement and support. Santosh acknowledges project support from DST (Government of India) to study fluid processes. This paper is a contribution to IGCP 348.

Received 5 September 1994, revised accepted 13 January 1995

Molecular modelling of N-terminal region of human cardiac myosin light chain 2 induced during cardiac hypertrophy

K. Kannan, G. Jegadeesh Babu[†], K. Veluraja[§] and C. Rajamanickam^{†,*}

Bioinformatics Centre, Department of Biotechnology, School of Biological Sciences, Madurai Kamaraj University, Madurai 625 021, India

[†]Department of Biochemistry, School of Biological Sciences, Madurai Kamaraj University, Madurai 625 021, India

[§]Physics Department, Manonmaniam Sundaranar University, Tirunelveli 627 002, India

Studies on the expression of phosphorylatable myosin light chain 2 (MLC2) in the cardiac tissues obtained from patients with various cardiac anomalies have shown an increased expression of MLC2 in both atrial and ventricular biopsy tissues of patients with atrial septal defect and ventricular septal defect. Also, in an attempt to predict the three-dimensional structure and to identify the site of phosphorylation of the N-terminal region of this inducible human cardiac MLC2, a model has been proposed based on computer analysis. The proposed model has indicated that this phosphorylatable N-terminal region falls in the helical conformation and the possible site of phosphorylation could be serine 19, which is at the centre of the helix and might be involved in the conformational changes during muscle contraction.

MYOSIN, one of the major constituents of muscle fibre, consists of two myosin heavy chains (MHC), two alkali light chains (MLC1) and two regulatory phosphorylatable myosin light chains (MLC2)¹. MLC2 has a characteristic hydrophobic head, as the N-terminal end, which binds to the actin during actomyosin complex formation. The regulation of myosin/actin interaction, crucial to force generation and enzymatic activity of myosin, is mediated by the regulatory light chains. MLC2 is phosphorylated by a Ca²⁺-stimulated light chain kinase and dephosphorylated by phosphatase C². Phosphorylation-induced changes of MLC2 are evident in smooth and skeletal muscles. Phosphorylation of smooth muscle MLC2 leads to contraction and dephosphorylation results in relaxation^{3,4}. In scallop adductor

muscle, MLC2 inhibits actin-activated myosin ATPase activity and this inhibition is relieved upon binding of calcium to myosin⁵. Removal of skeletal muscle MLC2 is known to cause a decrease in V_{max} of actin-activated myosin ATPase and its potentiation depends^{6,7} upon phosphorylation of MLC2. In cardiac muscle, the precise role of phosphorylation of MLC2 in myosin/actin interaction and subsequent ATPase activity is not known. The amino acid sequences derived from chicken, rat and human cardiac MLC2 genes share significant homology in the region of phosphorylatable serine and in the basic N-terminal region but are divergent in the C-terminal region⁸⁻¹⁰.

Recent studies have established that a significant increase occurs in MLC2 content and in the mRNA levels during myocardial hypertrophy in both rat and human¹¹⁻¹⁴. Unlike MHC, changes in α -actin isoforms have also been observed both in rat and human during cardiac hypertrophy. Thus, study of the role of MLC2 in actin/myosin interactions may suggest the underlying pathogenetic mechanisms during cardiac hypertrophy. Presently, in order to see whether MLC2 expression is induced invariably in all cardiac anomalies leading to hypertrophy, the expression of MLC2 in cardiac tissues of patients with hypertrophic heart in various cardiac disorders has been studied. These studies have demonstrated that the expression of MLC2 is induced in both atrial and ventricular tissues of patients with various cardiac anomalies.

This along with the information of sequence homology of the N-terminal region of cardiac MLC2 of rat and human led us to make an attempt on the structural studies of the phosphorylatable N-terminal region of MLC2 in order to gain an insight into the role of phosphoryla-

*For correspondence